

The importance of loading the periphery of the vertebral endplate

Joseph Cadman¹, Chester Sutterlin III^{2,3}, Danè Dabirrahmani¹, Richard Appleyard¹

¹Orthopaedic Biomechanics Group, Department of Biomedical Science, Faculty of Medicine and Health Science, Macquarie University, NSW, Australia; ²University of Florida, FL, USA; ³Spinal Health International, 511 Putter Lane, Longboat Key, FL, USA

Correspondence to: Joseph Cadman. Building F10A, Ground Floor, 2 Technology Place Macquarie University NSW, 2109, Australia.
Email: Joseph.cadman@mq.edu.au.

Background: Commercial fusion cages typically provide support in the central region of the endplate, failing to utilize the increased compressive strength around the periphery. This study demonstrates the increase in compressive strength that can be achieved if the bony periphery of the endplate is loaded.

Methods: Sixteen cadaveric lumbar vertebrae (L1–L5) were randomly divided into two even groups. A different commercial mass produced implant (MPI) was allocated to each group: (I) a Polyether-ether-ketone (PEEK) anterior lumbar inter-body fusion (ALIF) MPI; and (II) a titanium ALIF MPI. Uniaxial compression at a displacement rate of 0.5 mm/sec was applied to all vertebrae during two phases: (I) with the allocated MPI situated in the central region of the endplate; (II) with an aluminum plate, designed to load the bony periphery of the endplate. The failure load and mode of failure was recorded.

Results: From phase 1 to phase 2, the failure load increased from 1.1±0.4 to 2.9±1.4 kN for group 1; and from 1.3±1.0 to 3.0±1.9 kN for group 2. The increase in strength from phase 1 to phase 2 was statistically significant for each group (group 1: P<0.01, group 2: P<0.05, paired *t*-test). There was no significant difference between the groups in either phase (P>0.05, *t*-test). The mode of failure in phase 1 was the implant being forced through the endplate for both groups. In phase 2, the mode of failure was either a fracture of the epiphyseal rim or buckling of the side wall of the vertebral body.

Conclusions: Loading the periphery of the vertebral endplate achieved significant increase in compressive load capacity compared to loading the central region of the endplate. Clinically, this implies that patient-specific implants which load the periphery of the vertebral endplate could decrease the incidence of subsidence and improve surgical outcomes.

Keywords: Lumbar vertebrae; spinal fusion; biomechanical phenomena

Submitted Aug 01, 2016. Accepted for publication Sep 21, 2016.

doi: 10.21037/jss.2016.09.08

View this article at: <http://dx.doi.org/10.21037/jss.2016.09.08>

Introduction

Inter-body devices (IBDs) are commonly employed in spinal surgery for both immobilization procedures and motion preservation procedures. The former procedures commonly refer to fusion cages with bone graft; the latter procedures refer to total disc replacements.

There are a number of potential risks with the use of IBDs associated with: surgical approach (i.e., vascular, neurologic, organs); procedural problems (i.e., malposition of implant, suboptimal size of implant, damage to support structures, damage to stabilizing structures); patient

comorbidities (osteoporosis, malnutrition, smoking); and external events (trauma, accidental falls). In this study, we are concerned with clinical failures associated with mechanical failure, or implant subsidence through the endplate (*Figure 1*), due to anatomic restrictions or suboptimal sizing of the implant.

Subsidence rates in spinal fusion are reported as high as 30% (1). It is generally known that the bony periphery of the vertebral endplate possess greater compressive strength and stability than the central region (2–7). However, mass produced implants (MPIs) are not guaranteed to load the bony periphery of the endplate to provide optimum

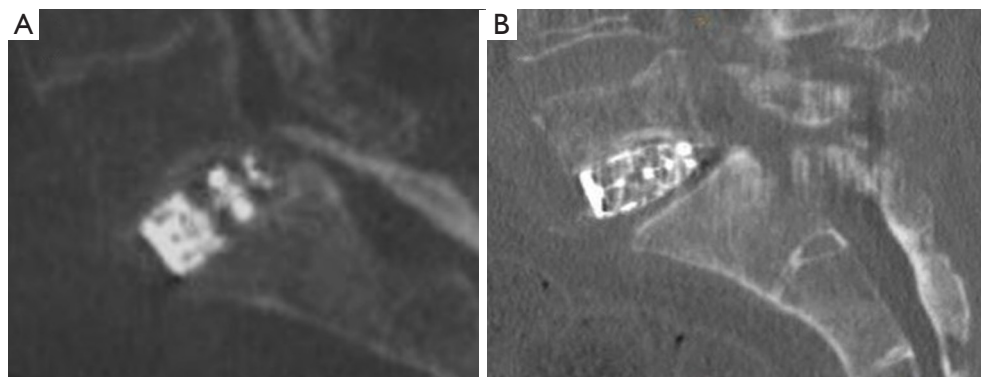


Figure 1 The use of a commercial MPI (A) immediately post-surgery and (B) following subsidence into the inferior endplate of L5.

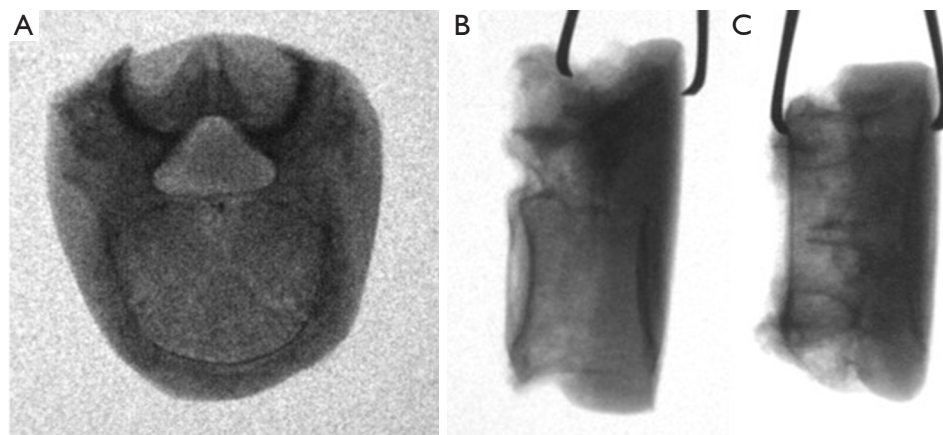


Figure 2 Fluoroscopic images showing (A) axial, (B) lateral and (C) AP views.

strength and stability. Indeed, anatomical access is always limited by the size of the portal created in the annulus fibrosis of the disc (6). Therefore, positioning the MPIs in the central region of the endplate is typically a less complicated procedure than ensuring that the endplate periphery is loaded, making this a common scenario (5). Supplemental fixation, either anteriorly, posteriorly or both is often used to provide the required stability (6,8).

Recently, moves have been made towards the use of patient specific implants (PSIs) for a range of procedures, including spinal fusion (9-12). Advances in CAD software and 3D printing technology have made it possible to produce PSIs with complex external and internal architecture (9,11,13). Utilizing this technology will permit the fabrication of spinal fusion PSIs which match the surface topology of the endplates precisely, ensuring ideal loading of the endplate periphery.

This paper aims to establish the difference in compressive

strength between the bony periphery and the central region of the vertebral endplate.

Methods

Sixteen cadaveric lumbar vertebrae were dissected and all soft tissue removed in accordance with ethics approval by Macquarie University (Ref. 5201300835). The vertebrae were harvested from 3 female donors with an average age of 83 years (range, 77–88 years) and 2 male donors with an average age of 88 years (range, 85–90 years). Although bone density was not measured, the age range would tend towards the worst case scenario of osteoporotic bone. The dimensions of the superior endplate of each vertebrae were measured. Fluoroscopy images were captured in order to exclude any specimens exhibiting defects (e.g., Schmorl's nodes) (Figure 2). The vertebrae were potted in cement (Trayplast NF, Vertex Dental, Zeist, Netherlands) for

stability (Figure 3).

The vertebrae were divided into two groups based on the type of MPI used in the testing. Group 1 used a 3D-printed titanium ALIF MPI (4WEB, size: W32 D20 H14 <math><12^\circ</math>) (Figure 4A); group 2 used PEEK ALIF MPI (K2M, size: W30 D24 H17 <math><5^\circ</math>) (Figure 4B). These MPI sizes were chosen based on the size of the 16 cadaveric vertebrae used in the study. An aluminum plate was also cut to match the profile of the largest vertebral endplate (Figure 4C). This was done to ensure that the whole endplate, including the bony periphery, would be loaded for all specimens.

Testing was completed in two phases. In phase 1, the commercial MPIs were used to load the endplate in a manner analogous to current surgical practice. These applied a compressive load on the central region of the endplate. In phase 2, all specimens from phase 1 were retested using the aluminum plate, which distributed the compressive load over the remaining bony periphery of the endplate. The specimens were maintained in the two



Figure 3 All vertebrae were potted in cement for stability.

groups described above, to allow the results to be paired for statistical analysis.

For testing, the MPI or aluminum plate were positioned on the superior endplate of the vertebra (Figure 3). Uniaxial compression was applied to all specimens at a constant displacement rate of 0.5 mm/s using an Instron E10000 electro-mechanical testing machine (Instron, Illinois, USA) equipped with a 10 kN load cell and a pair of compression plates (Figure 5). The failure load, defined as a significant deviation from linearity of the load-time curve, was recorded for each test (Figure 6). The mode of failure was also recorded.

A student *t*-test was used to determine the statistical significance of the failure results between the two groups at the end of each phase. Paired *t*-tests were used to determine the statistical significance between the implant and plate results within each group following phase 2. Results were considered statistically significant if $P < 0.05$.

Results

The dimensional data for the 16 vertebrae is presented in Table 1. The main dimensions of interest are the superior endplate dimensions. The average dimensions are reasonably small and the use of the small cages used would not be uncommon in a surgical scenario.

In phase 1, the failure loads were: 1.1 kN (S.D. =0.4 kN) for group 1 (PEEK cage) and 1.3 kN (S.D. =1.0 kN) for group 2 (titanium cage) (Figure 7). These values compare reasonably well to failure loads listed in the literature for similar testing protocols (3,4). There was no significant difference between the groups after phase 1 ($P > 0.05$).

In phase 2, when retesting with the aluminum plate, the

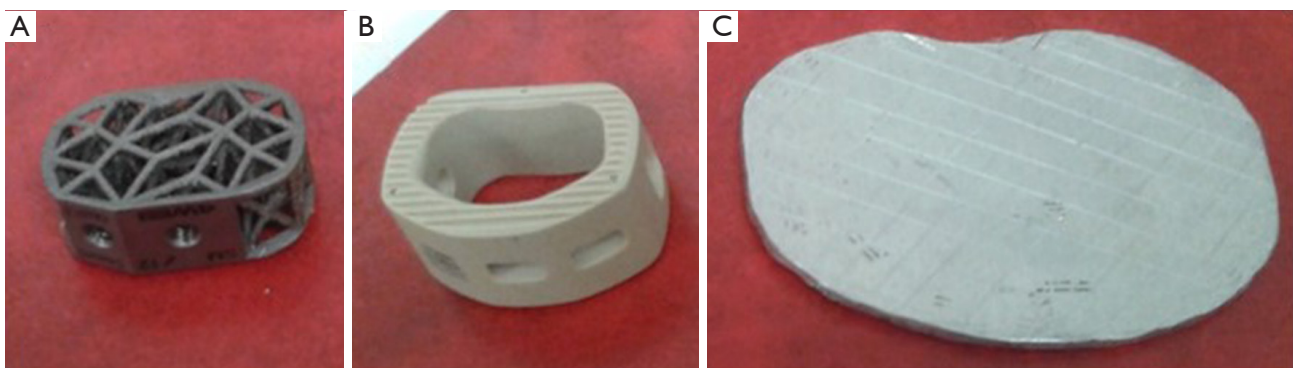


Figure 4 Commercial MPIs and plate used for testing including (A) titanium implant (4WEB), (B) PEEK implant (K2M) and (C) aluminum plate. MPI, mass produced implant; PEEK, Polyether-ether-ketone.

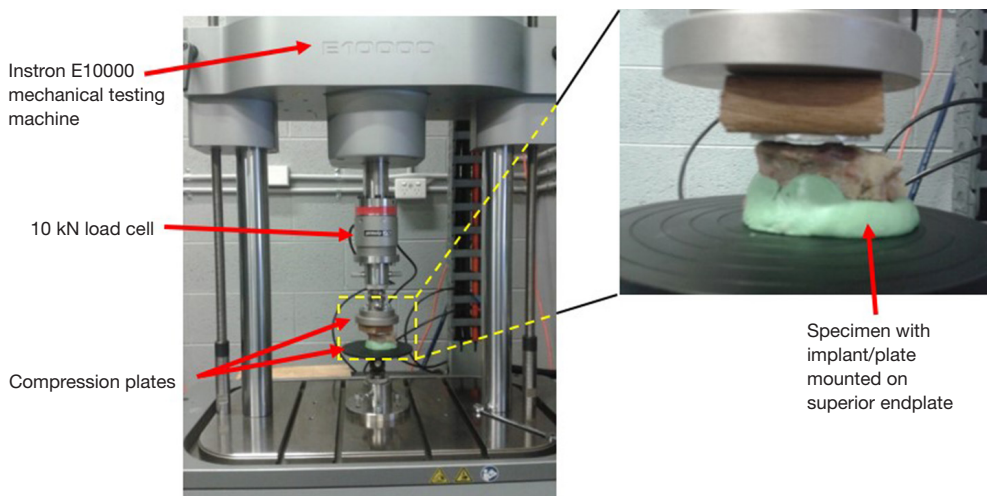


Figure 5 Uniaxial compression was applied using an Instron E10000 with a 10 kN load cell and compression plates. The specimen was mounted between the compression plates with the MPI or Aluminum plate mounted on the superior endplate.

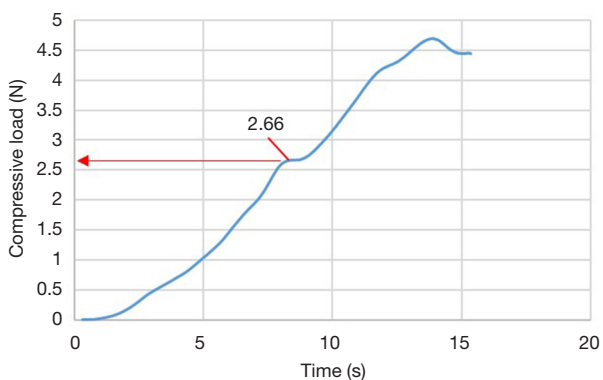


Figure 6 Sample load-time curve showing failure load as the first significant deviation from linearity.

failure load for group 1 increased from 1.1 kN (S.D. =0.4 kN) to 2.9kN (S.D. =1.4 kN); and from 1.3 kN (S.D. =1.0 kN) to 3.0 kN (S.D. =1.9 kN) (*Figure 7*). The increase in strength when retesting with the aluminum plate was statistically significant for each group (group 1: $P<0.01$, group 2: $P<0.05$, paired *t*-test). There was no significant difference between the groups following phase 2 ($P>0.05$, *t*-test).

The mode of failure for phase I for all specimens in both groups was the implant being forced through the endplate (*Figure 8A*). For phase II, when retested with the aluminum plate, the central region had already collapsed due to the earlier test. With the load supported only by the bony periphery, the mode of failure was either a fracture of the

Table 1 Average dimensions of harvested vertebrae

Level	Average width (range) (mm)	Average depth (range) (mm)	Average height (range) (mm)
L1	47.4 (39.9–52.5)	37.4 (35.4–39.7)	26.8 (23.6–31.1)
L2	48.2 (42.2–54.2)	35.9 (33.3–38.3)	29.9 (27.4–31.8)
L3	51.5 (43.7–61.1)	37.2 (32.0–43.9)	31.5 (26.7–35.8)
L4	59.0 (57.6–60.4)	40.5 (36.9–44.0)	32.0 (30.9–33.1)
L5	64.3 (62.9–65.7)	42.9 (40.1–45.6)	31.6 (31.3–31.8)

epiphyseal rim (Figure 8B) or buckling of the side wall of the vertebral body (Figure 8C).

Discussion

The average size of the vertebrae across the two groups was quite small (Table 1). The small MPIs chosen are commonly used sizes in the companies' implant sets. The age of the donors is also appropriate to the typical demographic requiring lumbar spinal fusion, although their advanced ages would tend towards osteoporosis and weakened bone strength.

For phase 1, the compressive failure loads between the two groups were very similar, with the titanium MPI being slightly higher. This is expected as the footprint for the two MPIs were similar. The slightly higher average failure load for the titanium MPI is due to the more even distribution

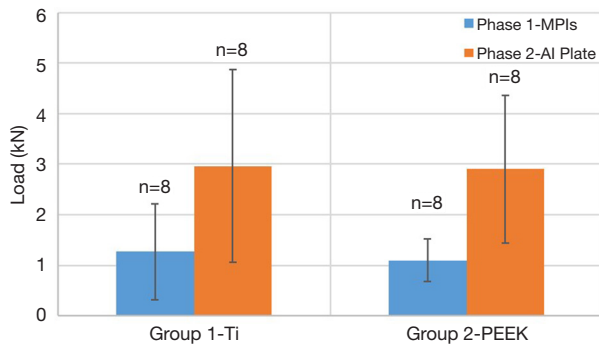


Figure 7 Average loads for both testing phases, showing phase 1 testing with the Ti or PEEK MPIs in blue and phase 2 resting with the aluminum plate orange.

of the load over the whole endplate. The failure mode for all of these specimens was the central region of the endplate collapsing into the vertebral body. The bony periphery was left intact for all specimens. This simulates the clinical situation and is known as subsidence. Therefore, all of the specimens were retested with the aluminum plate.

In phase 2, the average compressive load to failure for all the specimens in both groups increased to approximately 3 kN. This means that the bony periphery, without any additional support from the central endplate, provides resistance to approximately three times the compressive load than commercial MPIs that predominantly load the central region. Loading the periphery of the vertebral endplate increases the compressive load capacity of the vertebra via three avenues. Firstly, the walls of the vertebral body provide additional support in the direction of compression. Secondly, the extreme periphery of the endplate (epiphyseal rim) provides radial support, which permits a higher load to be resisted prior to failure. Finally, the bone density is greater in the epiphyseal rim, especially when longstanding degenerative disc disease produces sclerosis and osteophytes.

The MPIs failed by pushing the endplate into the vertebral body even when the MPI extended to the edges to the bony periphery, to the extent the epiphyseal rim sustains minor damage. For example, a small split in the epiphyseal rim can be seen on the right side of Figure 9A. An increase in compressive strength of 50% was still achieved in phase 2, when loading the remaining periphery in isolation (Figure 9B). This clearly shows that a custom designed implant, which accurately maps the profile of the epiphyseal rim could be the gold standard for inter-body fusion devices. It is important to emphasize that for phase 2, the central region of the endplate had already failed and

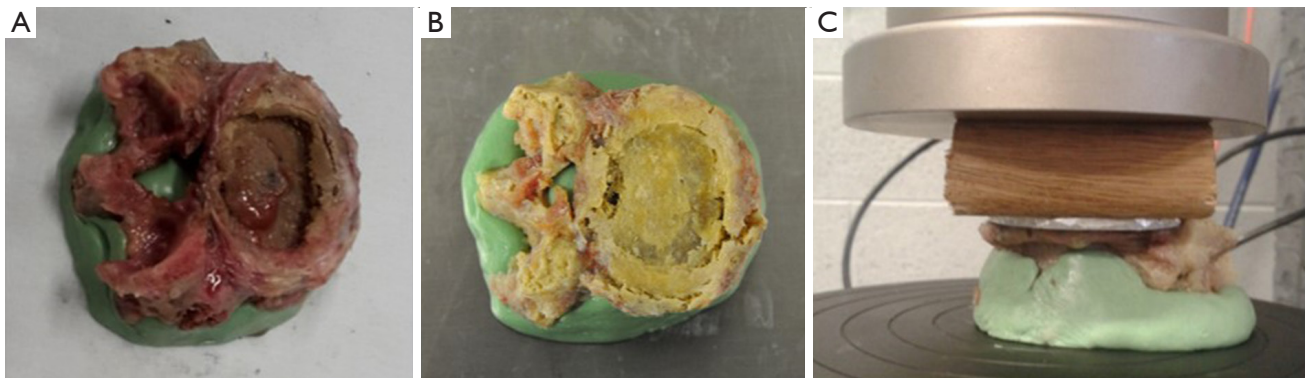


Figure 8 The modes of failure were (A) compressive failure of the MPI through the vertebral endplate in phase I, and either (B) fracture of the epiphyseal rim or (C) buckling of the side wall of the vertebral body in phase II. MPI, mass produced implant.

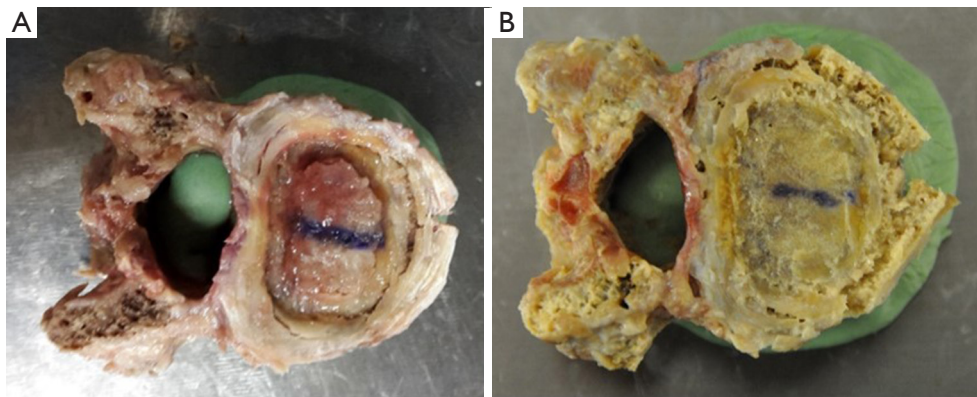


Figure 9 Even when the MPI covers the bulk of the endplate as in (A), retesting with the aluminum plate (B) causes the same mode of failure and, in this specific case, an increase in compressive strength of 50%. MPI, mass produced implant.

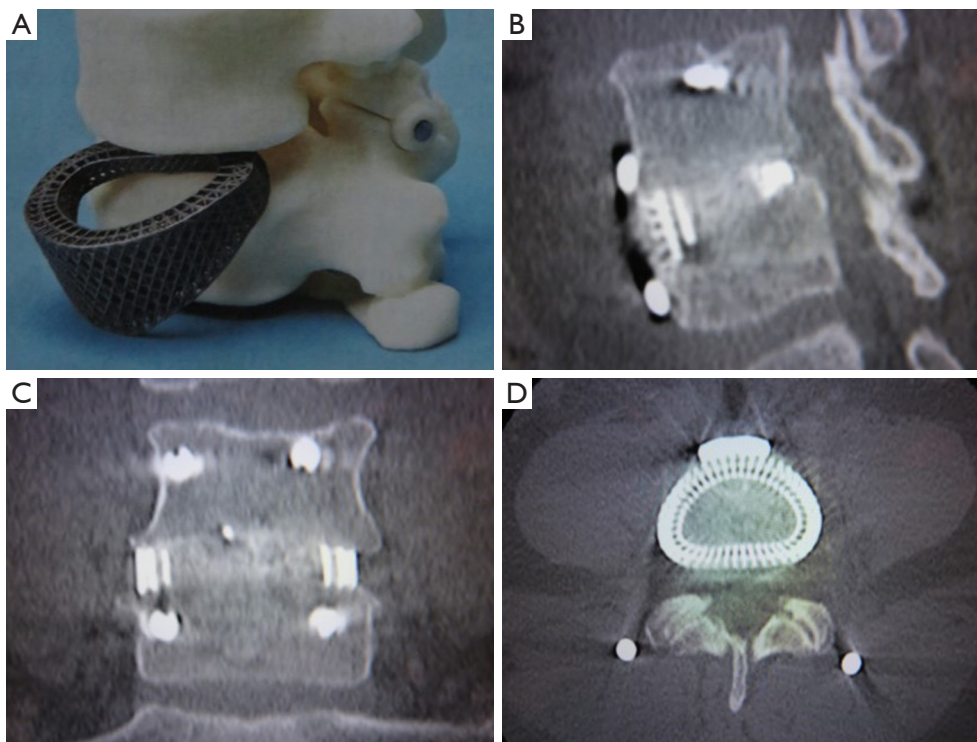


Figure 10 Clinical example of PSI showing (A) the PSI with a synthetic model of the patient spine, and 1 year post-operative CT images showing solid bony fusion between adjacent vertebrae in (A) lateral, (B) AP and (C) transverse cross-sections. PSI, patient specific implant.

provided no support during the subsequent compression loading with the aluminum plate.

In the clinical scenario, this study implies that patient-specific, customized implants which load the periphery of the vertebral endplate would decrease the incidence of subsidence and improve surgical outcomes. Indeed, 3D

printed PSIs designed to load the periphery of the vertebral endplate have been used clinically, with one-year follow-up scans showing that solid bony fusion has occurred through the center of the implant, between the two adjacent vertebral bodies (*Figure 10*).

There were several limitations to this study. Firstly,

bone mineral density (BMD) was not determined. Instead, specimens were harvested from donors in the appropriate demographic and fluoroscopy was used to eliminate specimens with defects. The fact that the average compressive failure load for the aluminum plate testing is similar over both groups indicates that the distribution of bone density and vertebra sizes are similar in both groups. Secondly, some of the vertebrae used in the test were larger and a larger MPI might have been selected during actual surgery. The use of the smaller MPI can be considered extreme in these instances. However, as noted above, there is still a significant increase in strength recorded for individual cases where the MPI would have been considered the appropriate size in a clinical scenario. Finally, the use of aluminum for the plate is not indicative of the types of material that are typically seen in surgical implants. However, for the purpose of this study (i.e., determining the effect of loading the epiphyseal rim in isolation), the choice of material is not likely to have an impact on the final results.

Acknowledgements

Funding: This study was funded by ProCRO Pty Ltd, which is registered to Chester SUTTERLIN III.

Footnote

Conflicts of Interest: The authors have no conflicts of interest to declare.

Ethical Statement: Sixteen cadaveric lumbar vertebrae were dissected and all soft tissue removed in accordance with ethics approval by Macquarie University (Ref. 5201300835) and written informed consent was obtained from all patients.

References

1. Marchi L, Abdala N, Oliveira L, et al. Radiographic and clinical evaluation of cage subsidence after stand-alone lateral interbody fusion. *J Neurosurg Spine* 2013;19:110-8.
2. Grant JP, Oxland TR, Dvorak MF. Mapping the structural properties of the lumbosacral vertebral endplates. *Spine (Phila Pa 1976)* 2001;26:889-96.
3. Tan JS, Bailey CS, Dvorak MF, et al. Interbody device shape and size are important to strengthen the vertebra-implant interface. *Spine (Phila Pa 1976)* 2005;30:638-44.
4. Steffen T, Tsantrizos A, Aebi M. Effect of implant design and endplate preparation on the compressive strength of interbody fusion constructs. *Spine (Phila Pa 1976)* 2000;25:1077-84.
5. Le TV, Baaj AA, Dakwar E, et al. Subsidence of polyetheretherketone intervertebral cages in minimally invasive lateral retroperitoneal transpsoas lumbar interbody fusion. *Spine (Phila Pa 1976)* 2012;37:1268-73.
6. Zhang JD, Poffyn B, Sys G, et al. Are stand-alone cages sufficient for anterior lumbar interbody fusion? *Orthop Surg* 2012;4:11-4.
7. Zander T, Rohlmann A, Klöckner C, et al. Effect of bone graft characteristics on the mechanical behavior of the lumbar spine. *J Biomech* 2002;35:491-7.
8. Deen HG, Fenton DS, Lamer TJ. Minimally invasive procedures for disorders of the lumbar spine. *Mayo Clin Proc* 2003;78:1249-56.
9. Hollister SJ, Flanagan CL, Zopf DA, et al. Design control for clinical translation of 3D printed modular scaffolds. *Ann Biomed Eng* 2015;43:774-86.
10. Chua MC, Chui CK. Optimization of Patient-Specific Design of Medical Implants for Manufacturing. *Procedia CIRP* 2016;40:402-6.
11. Stoor P, Suomalainen A, Lindqvist C, et al. Rapid prototyped patient specific implants for reconstruction of orbital wall defects. *J Craniomaxillofac Surg* 2014;42:1644-9.
12. Sutradhar A, Park J, Carrau D, et al. Designing patient-specific 3D printed craniofacial implants using a novel topology optimization method. *Med Biol Eng Comput* 2016;54:1123-35.
13. Nassau CJ, Litofsky NS, Lin Y. Analysis of spinal lumbar interbody fusion cage subsidence using Taguchi method, finite element analysis, and artificial neural network. *Front Mech Eng* 2012;7:247-55.

Contributions: (I) Conception and design: C Sutterlin III; (II) Administrative support: None; (III) Provision of study materials or patients: J Cadman, D Dabirrahmani; (IV) Collection and assembly of data: J Cadman; (V) Data analysis and interpretation: J Cadman; (VI) Manuscript writing: All authors; (VII) Final approval of manuscript: All authors.

Cite this article as: Cadman J, Sutterlin C 3rd, Dabirrahmani D, Appleyard R. The importance of loading the periphery of the vertebral endplate. *J Spine Surg* 2016;2(3):178-184. doi: 10.21037/jss.2016.09.08